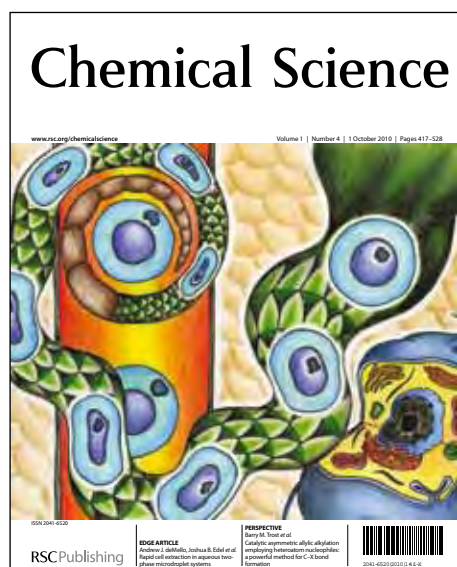


# Chemical Science

Accepted Manuscript



This is an *Accepted Manuscript*, which has been through the RSC Publishing peer review process and has been accepted for publication.

*Accepted Manuscripts* are published online shortly after acceptance, which is prior to technical editing, formatting and proof reading. This free service from RSC Publishing allows authors to make their results available to the community, in citable form, before publication of the edited article. This *Accepted Manuscript* will be replaced by the edited and formatted *Advance Article* as soon as this is available.

To cite this manuscript please use its permanent Digital Object Identifier (DOI®), which is identical for all formats of publication.

More information about *Accepted Manuscripts* can be found in the [Information for Authors](#).

Please note that technical editing may introduce minor changes to the text and/or graphics contained in the manuscript submitted by the author(s) which may alter content, and that the standard [Terms & Conditions](#) and the [ethical guidelines](#) that apply to the journal are still applicable. In no event shall the RSC be held responsible for any errors or omissions in these *Accepted Manuscript* manuscripts or any consequences arising from the use of any information contained in them.

## ARTICLE

## Organic-Inorganic Hybrid Polyhedra That Can Serve as Supramolecular Building Blocks

Cite this: DOI: 10.1039/x0xx00000x

Zhenjie Zhang, Lukasz Wojtas and Michael J. Zaworotko\*

Received 00th October 2013,  
Accepted 00th November 2013

DOI: 10.1039/x0xx00000x

www.rsc.org/

## Introduction

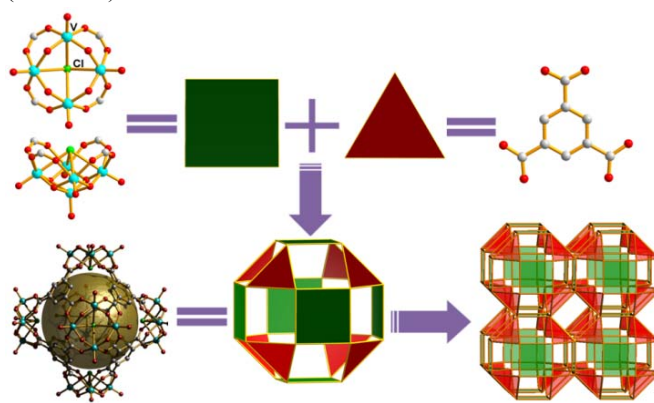
The modular nature of metal-organic materials (MOMs) that results in their structural and functional diversity means that MOMs have attracted intense research activity over the past two decades.<sup>1</sup> MOMs that are sustained by nanoscale polyhedral building blocks (nanoballs) that in effect serve as supermolecular building blocks, SBBs, are an important subset of MOMs and they include extra-large surface area materials with surface areas up to 10,000 m<sup>2</sup>/g.<sup>2</sup> Such MOMs enable studies that take advantage of porosity in the context of gas sorption,<sup>3</sup> drug delivery<sup>4</sup> and catalysis.<sup>5</sup> Such MOMs take advantage of the symmetry and exterior functionality of nanoballs by exploiting them as SBBs that are cross-linked by organic ligands or metal moieties.<sup>6</sup> For example, the prototypical nanoball is based upon square paddlewheel moieties that are linked at their vertices by 1,3-benzenedicarboxylate anions to form a discrete *small rhombihexahedron*.<sup>7</sup> This nanoball has been exploited as an SBB to form **tbo**,<sup>8</sup> **rht**<sup>9</sup> and **pcu**<sup>10</sup> nets. MOMs that are based upon polyhedral nanoballs are most typically synthesized via one-pot processes.<sup>11</sup> However, Zhou *et al.*<sup>12</sup> and Su *et al.*<sup>13</sup> recently reported isolation of nanoballs before cross-linking with 4,4'-bipyridine to form **pcu** and **fcu** nets, respectively.

Polyoxometalates (POMs) are exemplified by soluble anionic high oxidation state metal oxide clusters of d-block transition metals (especially W<sup>VI</sup>, Mo<sup>V,VI</sup> and V<sup>IV,V</sup>) and have also attracted considerable attention for their structure and properties.<sup>14</sup> In the context of MOMs, POMs have been used as nodes to generate polyoxometalate metal-organic frameworks (POMOFs)<sup>15</sup> or encapsulated as guests (POM@MOFs).<sup>16</sup> However, although POM nanoballs based upon regular polyhedra have been reported, they are purely inorganic as they are sustained by O-M-O bonds.<sup>17</sup> Organic-inorganic hybrid nanoballs (**hyballs**) in which POMs serve as molecular building blocks (MBBs) that are linked by organic ligands to form polyhedra remain underexplored. Indeed, we are aware of only two examples: Schmitt's POM capsule (**hyball-1**) formed from a POM and organoarsenic or phosphonic acids;<sup>18a,b</sup> Yang's cube from Ni<sub>6</sub>-POMs linked by 1,3,5-benzenetricarboxylate (BTC) (**hyball-2**).<sup>18c</sup>

In this contribution, we introduce a third class of **hyball** based upon well-known<sup>19,20</sup> POMs with carboxylate ligands at their

[V<sub>4</sub>O<sub>8</sub>X(COO)<sub>4</sub>]<sup>z-</sup> or [V<sub>5</sub>O<sub>9</sub>X(COO)<sub>4</sub>]<sup>2-</sup> polyoxometalate anions can function as 4-connected nodes that assemble with 3-connected organic nodes (1,3,5-benzenetricarboxylate) to afford *small cubicoctahedral* hybrid nanoballs (**hyball-3**, **-4**, **-5**) in high yield. The resulting polyhedral cages exhibit 550 Å<sup>3</sup> internal volumes and gas sorption measurements reveal that solid forms of the **hyballs** are permanently porous. The exterior surfaces of the **hyballs** are suited for further self-assembly and **hyball-3** can serve as an octahedral supermolecular building block for the generation of primitive cubic (**pcu**) nets *via* two types of linkage: hydrogen bonds or coordination bonds.

periphery. These shuttlecock-like vanadium POMs, V-POMs, [V<sub>4</sub>O<sub>8</sub>X(COO)<sub>4</sub>]<sup>z-</sup> (X = Cl<sup>-</sup>, Br<sup>-</sup>, NO<sub>3</sub><sup>-</sup> and K<sup>+</sup>; z = 1 or 2) and [V<sub>5</sub>O<sub>9</sub>X(COO)<sub>4</sub>]<sup>2-</sup>, are suited to sustain *cubicoctahedral* nanoballs since V-POMs and BTC can serve as square and triangular faces, respectively (Scheme 1). They therefore follow one of the three design principles that have been successfully applied to nanoballs: vertex-directed,<sup>21</sup> face-directed (molecular paneling);<sup>22,23</sup> edge directed<sup>22</sup> self-assembly. These approaches afford polyhedra with windows and faces, faces only or windows only, respectively. Herein we address the use of V-POMs as square MBBs that are vertex-linked by 3-connected 1,3,5-benzenetricarboxylate, BTC, anions. The resulting *small cubicoctahedral* **hyballs** (**hyball-3**, **-4**, **-5**) can in turn serve as SBBs for the generation augmented **pcu** nets (Scheme 1).



**Scheme 1.** **Hyball-3**, **-4** and **-5** are comprised of eight triangular faces (3-connected BTC anions) and six square faces (4-connected V-POMs) that are vertex-linked so as to form a *small cubicoctahedron*; **Hyball-3** can serve as a 6-connected octahedral SBB to afford augmented **pcu** nets *via* coordination bonding or hydrogen bonding at its square faces.

## Results and discussion

Reaction of H<sub>3</sub>BTC with VCl<sub>3</sub> in N,N-dimethylacetamide (DMA) and H<sub>2</sub>O affords dark green rhombic crystals of **hyball-3**: (NH<sub>2</sub>Me<sub>2</sub>)<sub>6</sub>[(V<sub>4</sub>O<sub>8</sub>Cl)<sub>6</sub>(BTC)<sub>8</sub>].[Solvent] (Solvent = DMA, H<sub>2</sub>O). Single crystal x-ray diffraction (SCXRD) revealed that **hyball-3** adopts the tetragonal space group *I4/m* with *a* = *b* = 21.1256(6) Å and *c* = 27.4118(14) Å. **Hyball-3** is comprised of six tetranuclear [V<sub>4</sub>O<sub>8</sub>Cl(COO)<sub>4</sub>]<sup>1-</sup> MBBs linked by eight triangular BTC ligands (Fig. 1a). Each vanadium cation exhibits octahedral geometry through two μ<sub>2</sub>-η<sup>1</sup>η<sup>1</sup> carboxylate moieties, two μ<sub>2</sub>-O<sup>2-</sup> ligands, one terminal O<sup>2-</sup> ligand and one μ<sub>4</sub>-Cl ligand. The -6 charge of each **Hyball-3** anion is balanced by six [NH<sub>2</sub>Me<sub>2</sub>]<sup>+</sup> cations (there are six monoanionic [V<sub>4</sub>O<sub>8</sub>Cl(COO)<sub>4</sub>]<sup>1-</sup> MBBs per **hyball-3**). Fig. S1 reveals that V1, V2, V3 and V4 are assigned to be V<sup>V</sup> with V=O bond distances ranging from 1.591(4) to 1.602(4) Å and V-O bond distances from 1.794(3) to 2.042(3) Å.<sup>24</sup> The μ<sub>4</sub>-Cl moiety caps a square pyramid with V-Cl bonds of 2.795(5) to 2.852(1) Å. Bond valence sum (BVS) calculations<sup>25</sup> (Table S1) support V<sup>V</sup>, as does a previous report.<sup>20</sup> **Hyball-3** has an outer diameter of ~20 Å, and an inner diameter of ~14 Å. The estimated internal volume of **hyball-3** is ~550 Å<sup>3</sup> but its windows are too small to allow ingress and egress (1.0 Å × 2.3 Å after subtracting *van der Waals* radii). Each **hyball** is connected to four adjacent **hyballs** by two [NH<sub>2</sub>Me<sub>2</sub>]<sup>+</sup> cations to form an H-bonded 2D square grid net *via* charge assisted O<sup>-</sup>⋯H-N-H<sup>+</sup>⋯O hydrogen bonds (Fig. 2 left and Fig. S2). The 2D H-bonded layers stack in ABAB fashion along the *c* direction. The A-A distance between square grid layers is 11.8 Å (the nearest V<sup>V</sup>⋯V<sup>V</sup> distance). There are free [NH<sub>2</sub>Me<sub>2</sub>]<sup>+</sup> cations and solvent molecules located within the H-bonded layers to balance the extra charge for each **hyball** and fill the pore spaces. Crystals of **hyball-3** were observed to undergo a phase change to a new crystalline phase, **hyball-3'**, when exposed to the atmosphere for 2 weeks. SCXRD revealed that **hyball-3'** adopts the tetragonal space group *P4/n* with *a* = *b* = 21.049(1) Å and *c* = 21.633(4) Å. As shown in Fig. S2 and S3, an overall comparison of the **hyball** packing in **hyball-3'** and **hyball-3** revealed that there were only slight differences between the two structures in the *ab* plane as **hyball-3'** forms a H-bonded square grids similar to those observed in the *ab* plane of **hyball-3** (Fig. S3). However, the **hyballs** pack much closer along the *c* direction with the distance between square grid layers shrinking from 11.8 to 6.1 Å in **hyball-3'** because of a rearrangement of [NH<sub>2</sub>Me<sub>2</sub>]<sup>+</sup> cations in the pores. This rearrangement means that A-layers are now cross-linked along the *c* direction by V-O<sup>-</sup>⋯H-N-H<sup>+</sup>⋯O-V hydrogen bonds from [NH<sub>2</sub>Me<sub>2</sub>]<sup>+</sup> cations. The resulting architecture can be described as an H-bonded **pcu** net (Fig. 2, right). B-layers are likewise cross-linked to produce a doubly interpenetrated **pcu** network.

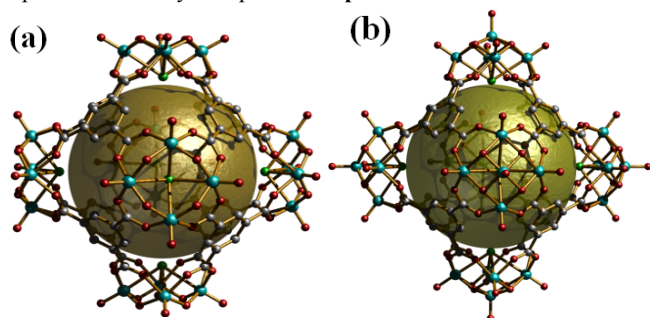


Fig. 1. The structures of (a) **hyball-3** and (b) **hyball-4**.

The same conditions used to prepare **hyball-3** but with N,N-dibutylformamide (DBF)/H<sub>2</sub>O as solvent afforded **hyball-4**, (NH<sub>2</sub>(Butyl)<sub>2</sub>)<sub>12</sub>[(V<sub>5</sub>O<sub>9</sub>Cl)<sub>6</sub>(BTC)<sub>8</sub>].[Solvent]. SCXRD revealed that **hyball-4** crystallizes in the rhombohedral space group *R-3c* with *a* = *b* = 34.773(3) Å and *c* = 39.676(3) Å. **Hyball-4** consists of 6

pentanuclear [V<sub>5</sub>O<sub>9</sub>Cl(COO)<sub>4</sub>]<sup>2-</sup> clusters linked by 8 BTC ligands (Fig. 1b). A V<sup>V</sup> cation is located above four basal V<sup>IV</sup> cations (Fig. S4). The oxidation states for the vanadium cations are consistent with previous reports<sup>20a,26</sup> and further supported by BSV calculations as detailed in Table S2. The apical V<sup>V</sup> atom is five-coordinate and adopts square pyramidal geometry through four μ<sub>2</sub>-O<sup>2-</sup> and one terminal O<sup>2-</sup> anion. V=O bond distances range from 1.572(9) to 1.594(9) Å while V-O bond distances range from 1.836(9) to 2.036(10) Å. The existence of **hyballs** with either tetranuclear [V<sub>4</sub>O<sub>8</sub>X(COO)<sub>4</sub>]<sup>z-</sup> or pentanuclear [V<sub>5</sub>O<sub>9</sub>Cl(COO)<sub>4</sub>]<sup>2-</sup> MBBs prompted us to explore whether mixed MBBs might also result in **hyballs**. This was indeed accomplished by increasing the proportion of VCl<sub>3</sub> used in the synthesis of **hyball-3**, thereby affording dark green rhombic crystals of **hyball-5** of a formula (NH<sub>2</sub>Me<sub>2</sub>)<sub>8</sub>[(V<sub>4</sub>O<sub>8</sub>Cl)<sub>3.8</sub>(V<sub>5</sub>O<sub>9</sub>Cl)<sub>2.2</sub>(BTC)<sub>8</sub>].[Solvent]. The formula was determined by refinement of the site occupancy factor of the V<sup>V</sup> moiety. In **hyball-5** the ratio of tetranuclear [V<sub>4</sub>O<sub>8</sub>X(COO)<sub>4</sub>]<sup>z-</sup> to pentanuclear [V<sub>5</sub>O<sub>9</sub>Cl(COO)<sub>4</sub>]<sup>2-</sup> MBBs is ca. 3.8/2.2. **Hyball-5** (*I4/m*, *a* = *b* = 21.1683(5) Å and *c* = 27.3991(15) Å) is isostructural with **hyball-3**.

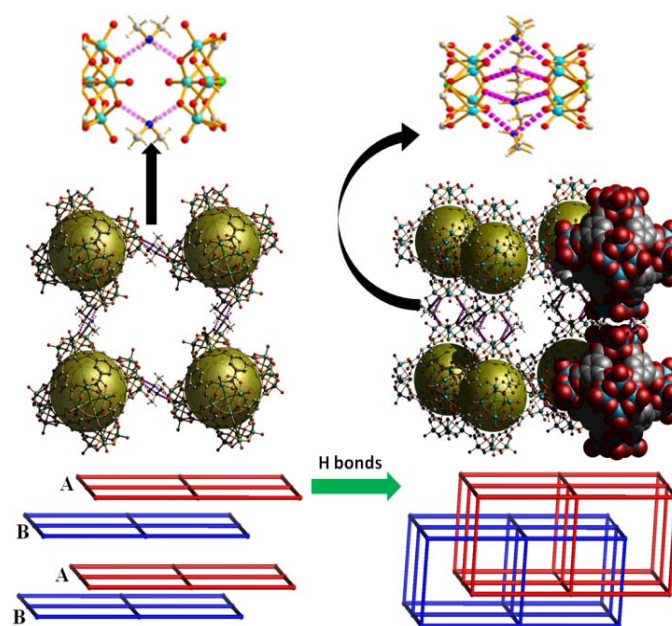
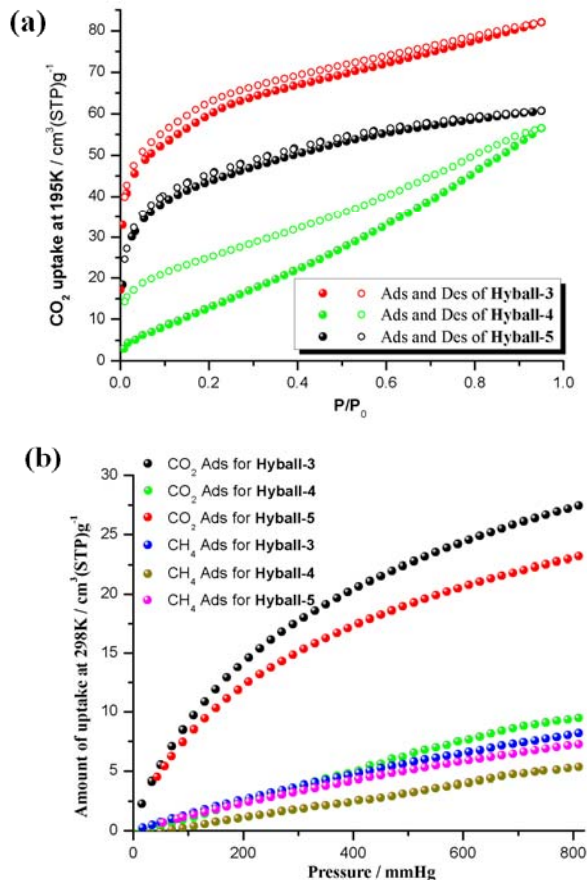


Fig. 2. The H-bonded 2D square grid net (left, viewed looking at the *ab* plane) of **Hyball-3** converts to **Hyball-3'**, a doubly interpenetrated **pcu** net, upon exposure to air for 2 weeks (right).

**Hyball-3**, -4 and -5 were activated for gas sorption studies by exchanging with MeOH for three days and then heating at 60 °C for 10 h under vacuum. The powder X-ray diffraction patterns (PXRDs) of **hyball-3** and -5 measured after activation were found to closely match those of **hyball-3'** indicating that removal of guest solvent molecules promote the phase change **hyball-3** to **hyball-3'**. All three materials were found to be permanently porous following activation. Gas sorption studies revealed that **hyball-3**, -4 and -5 adsorb CO<sub>2</sub> with uptakes of 82.0, 56.5 and 60.7 cm<sup>3</sup>/g respectively at 195K and P/P<sub>0</sub> = 0.95, corresponding to Langmuir surface areas (calculated from the pressure region 10-100 mmHg) of 313.2, 56.0 and 199.4 m<sup>2</sup>/g, respectively (Fig. 3a). Fig. 3b presents the CO<sub>2</sub> gravimetric uptake at 298 K and 1 atm, which were observed to be 27.0, 9.1 and 22.6 cm<sup>3</sup>/g for **hyball-3**, -4 and -5 respectively. As shown in Fig. S5, **hyball-3** and -5 exhibit type I N<sub>2</sub> sorption isotherms with uptakes of 74.0 and 61.4 cm<sup>3</sup>/g at 77K and P/P<sub>0</sub>=0.95 whereas **hyball-4** was found to be non-porous with respect to N<sub>2</sub>. The observed porosity

can be ascribed to be the interstitial spaces between adjacent hyballs since the windows ( $\sim 1.0 \text{ \AA} \times 2.3 \text{ \AA}$ ) of the hyballs are too small to allow passage of  $\text{N}_2$  or  $\text{CO}_2$ .<sup>27</sup> The isosteric heat of adsorption ( $Q_{st}$ ) for  $\text{CO}_2$  was calculated using the virial method from  $\text{CO}_2$  isotherms collected at 273 and 298 K (Fig. S6). **Hyball-3**, **-4** and **-5** exhibit  $Q_{st}$  for  $\text{CO}_2$  of 28.8, 24.4 and 33.2 kJ/mol, respectively, at zero coverage. IAST calculations<sup>28</sup> based on the experimental  $\text{CO}_2$  and  $\text{CH}_4$  isotherms at 298K suggest initial  $\text{CO}_2/\text{CH}_4$  selectivities of 7.7, 2.0 and 7.6 for **hyball-3**, **-4** and **-5**, respectively (Fig. S7).



**Fig. 3.** Gas adsorption isotherms for **hyball-3**, **-4** and **-5**: (a)  $\text{CO}_2$  at 195K; (b)  $\text{CO}_2$  at 298K and  $\text{CH}_4$  at 298K.

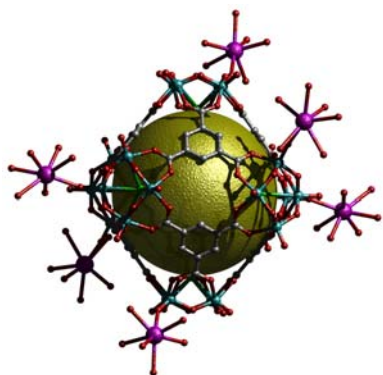


**Fig. 4.** Each hyball is cross-linked by six  $\text{Ba}^{2+}$  cations in **hyball-3-Ba**.

The peripheral portions of the polyoxovanadate clusters in **hyball-3** are rich in oxygen atoms that are oriented in such a manner that a

concave surface exists for each MBB. This surface seems well-suited to coordinate with metal cations. Further, **hyball-3** is anionic and soluble in polar solvents like  $\text{H}_2\text{O}$ , dimethylformide (DMF), DMA and dimethyl sulfoxide (DMSO). We therefore explored if **hyball-3** can indeed serve as an SBB in network structures when a 2-step synthetic strategy<sup>12,13</sup> is applied. Dissolution of **hyball-3** in DMA/ $\text{H}_2\text{O}$  resulted in a dark green solution and layering of this solution with  $\text{BaCl}_2$  in MeOH for one week afforded hexagonal green crystals of  $(\text{Ba}(\text{Solvent})_8)_2[(\text{V}_4\text{O}_8\text{Cl})_6(\text{BTC})_8\text{Ba}_3(\text{Solvent})_{15}][\text{Solvent}]$ , **hyball-3-Ba**. **Hyball-3-Ba** crystallizes in the monoclinic  $C2/c$  space group with a unit cell of  $a = 37.3416(11) \text{ \AA}$ ,  $b = 21.5080(6) \text{ \AA}$ ,  $c = 36.8796(10) \text{ \AA}$ ,  $\alpha = \gamma = 90^\circ$  and  $\beta = 109.771(1)^\circ$ . Conversely, a one-pot reaction of  $\text{VCl}_3$ ,  $\text{H}_3\text{BTC}$  and  $\text{BaCl}_2$  produced a yellowish-green solution but no crystals. A SCXRD study was conducted upon **hyball-3-Ba** and revealed that it is an augmented **pcu** (**pcu-a**) network in which each **hyball** serves as a 6-connected octahedral SBB linked by  $\text{V}=\text{O}-\text{Ba}-\text{O}=\text{V}$  bridges (Fig. 4). The resulting polyhedron based net is as depicted in Scheme 1. Fig. 5 reveals that hyballs are connected by seven-coordinated  $\text{Ba}^{2+}$  ions to produce a square grid net along the  $bc$  plane. These square grid nets are further cross-linked by bridging  $\text{Ba}^{2+}$  ions along the  $a$  direction to form an augmented **pcu** net.  $[\text{Ba}(\text{solvent})_8]^{2+}$  cations lie in the channels to balance the negatively charged  $[(\text{V}_4\text{O}_8\text{Cl})_6(\text{BTC})_8\text{Ba}_3(\text{Solvent})_{12}]^{4-}$  framework.  $\text{V}=\text{O}$  bond distances range from 1.570(8) to 1.596(5)  $\text{ \AA}$  and  $\text{V}-\text{O}$  bond distances range from 1.830(9) to 2.038 (10)  $\text{ \AA}$ .  $\text{Ba}-\text{O}$  bonds exhibit an average distance of 2.901(2)  $\text{ \AA}$ , which is within expected values.<sup>29</sup> **Hyball-3-Ba** was activated for gas adsorption using a similar procedure to that used for **hyball-3** and  $\text{N}_2$  and  $\text{CO}_2$  were tested to evaluate its porosity. At 77K and  $P/P_0 = 0.95$ , **Hyball-3-Ba** exhibits  $\text{N}_2$  uptake (Fig. S8) of 35.8  $\text{cm}^3/\text{g}$  that corresponds to a Langmuir surface area of 113.8  $\text{m}^2/\text{g}$ .  $\text{CO}_2$  gravimetric uptake for **Hyball-3-Ba** was (a) rved to be 26.0  $\text{cm}^3/\text{g}$  at 298 K and 1 atm (Fig. S9).

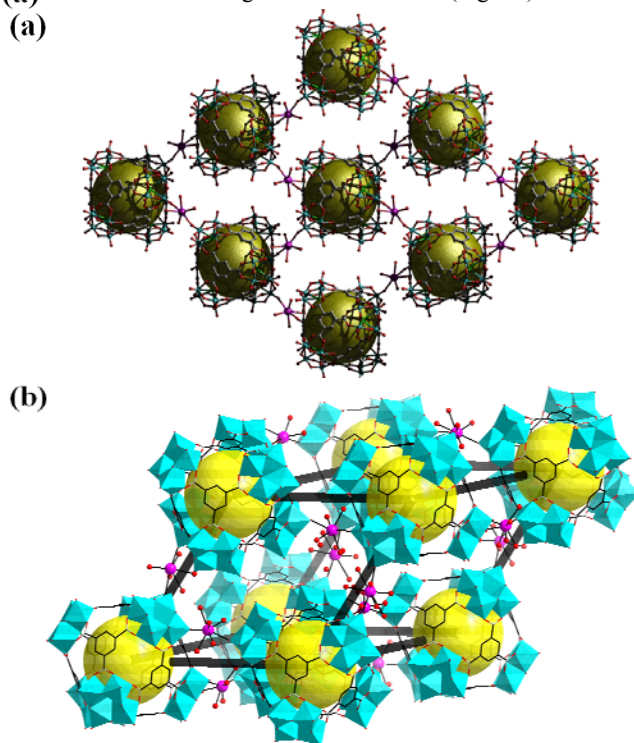


**Fig. 5.** (a) Hyballs in **hyball-3-Ba** are connected by  $\text{Ba}^{2+}$  ions to form a square grid net along the  $bc$  plane; (b) these square grid nets are further linked by  $\text{Ba}^{2+}$  cations to produce a **pcu** network (highlighted by black lines,  $\text{Ba}^{2+}$  pink,  $\text{V}$ , turquoise).

## Conclusions

In conclusion, we have demonstrated that BTC self-assembles with tetranuclear and pentanuclear V-POMs to form a new family of hybrid nanoball structures (**hyballs**), **Hyball-3**, **-4**, **-5**. These **hyballs** are robust, permanently porous and their exterior surfaces facilitate cross-linking to generate **pcu** nets. Such materials are likely to exhibit promise as catalysts or biosensors and are being further investigated in our laboratory in this context.

## Acknowledgements

Data for **hyball-3** were collected at the Advanced Photon Source on beamline 15ID-C of ChemMatCARS Sector 15, which is principally supported by the National Science Foundation/Department of Energy under grant number NSF/CHE-0822838. The Advanced Photon Source is supported by the U. S. Department of Energy, Office of Science, Office of Basic Energy Sciences, under Contract No. DE-AC02-06CH11357. We thank Prof. Peng Cheng, Prof. Wei Shi and Zheng Niu from Nankai University for their assistance in crystal data collection.

## Notes and references

Department of Chemistry, University of South Florida, 4202 East Fowler Avenue, CHE205, Tampa, FL33620, USA

E-mail: xtal@usf.edu

†Electronic supplementary information (ESI) available: experimental sections, PXRD, TGA, gas sorption, CO<sub>2</sub>/CH<sub>4</sub> selectivity, crystal supporting figures, tables of BVS calculation, and CCDC 965262 to 965266. For ESI and crystallographic data in CIF or other electronic format see DOI:10.1039/x0xx00000x.

- (1) S. R. Batten, S. M. Neville and D. R. Turner, *Coordination Polymers: Design, Analysis and Application*; Royal Society of Chemistry, Cambridge, UK, 2009.
- (2) L. R. MacGillivray, Ed. *Metal-Organic Frameworks: Design and Application*; Wiley & Sons, Inc., Hoboken, New Jersey, USA, 2010.
- (3) (a) O. K. Farha, I. Eryazici, N. C. Jeong, B. G. Hauser, A. A. Sarjeant, S. T. Nguyen, A. Ö. Yazaydin and J. T. Hupp, *J. Am. Chem. Soc.* 2012, **134**, 15016.
- (4) (a) O. K. Farha, A. Ö. Yazaydin, I. Eryazici, B. G. Mallakas, B. G. Hauser, M. G. Kanatzidis, S. T. Nguyen, R. Q. Snurr and J. T. Hupp, *Nat. Chem.* 2010, **2**, 944; (b) J.-R. Li, Y. Ma, M. C. McCarthy, J. Sculley, J. Yu, H.-K. Jeong, P. B. Balbuena and H.-C. Zhou, *Coord. Chem. Rev.* 2011, **255**, 1791.
- (5) P. Horcajada, C. Serre, G. Maurin, N. A. Ramsahye, F. Balas, M. Vallet-Regi, M. Sebban, F. Taulelle and G. Férey, *J. Am. Chem. Soc.* 2008, **130**, 6774; (b) R. C. Huxford, J. D. Rocca and W. Lin, *Curr Opin Chem Biol.* 2010, **14**, 262.
- (6) J. Lee, O. K. Farha, J. Roberts, K. A. Scheidt, S. T. Nguyen and J. T. Hupp, *Chem. Soc. Rev.* 2009, **38**, 1450.
- (7) (a) B. Moulton, J. J. Lu, A. Mondal and M. J. Zaworotko, *Chem. Commun.* 2001, 863; (b) M. Eddaoudi, J. Kim, J. B. Wachter, H. K. Chae, M. O'Keeffe and O. M. Yaghi, *J. Am. Chem. Soc.* 2001, **123**, 4368.
- (8) S. S.-Y. Chui, S. M.-F. Lo, J. P. H. Charmant, A. G. Orpen and I. D. Williams, *Science* 1999, **283**, 1148.
- (9) F. Nouar, J. F. Eubank, T. Bousquet, L. Wojtas, M. J. Zaworotko and M. Eddaoudi, *J. Am. Chem. Soc.* 2008, **130**, 1833.
- (10) J. J. Perry, V. C. Kravtsov, G. J. McManus, M. J. Zaworotko, *J. Am. Chem. Soc.* 2007, **129**, 10076.
- (11) N. Stock and S. Biswas, *Chem. Rev.* 2012, **112**, 933.
- (12) J.-R. Li, A. Yakovenko, W. Lu, D. J. Timmons, W. Zhuang, D. Yuan and H.-C. Zhou, *J. Am. Chem. Soc.* 2010, **132**, 17599.
- (13) H.-N. Wang, X. Meng, G.-S. Yang, X.-L. Wang, K.-Z. Shao, Z.-M. Su and C.-G. Wang, *Chem. Commun.* 2011, **47**, 7128.
- (14) *Thematic Issue on Polyoxometalates*, *Chem. Rev.* 1998, **98**, 1.
- (15) B. Nohra, H. E. Moll, M. R. Albelo, P. Mialane, J. Marrot, C. Mellot-Draznieks, M. O'Keeffe, R. N. Biboum, J. Lemaire, B. Keita, L. Nadjo and A. Dolbecq, *J. Am. Chem. Soc.* 2012, **133**, 13363.
- (16) (a) J. Song, Z. Luo, D. K. Britt, H. Furukawa, O. M. Yaghi, K. I. Hardcastle and C. L. Hill, *J. Am. Chem. Soc.* 2011, **133**, 16839; (b) C.-Y. Sun, S.-X. Liu, D.-D. Liang, K.-Z. Shao, Y.-H. Ren, Z.-M. Su, *J. Am. Chem. Soc.* 2009, **131**, 1883.
- (17) (a) L. Zhang and W. Schmitt, *J. Am. Chem. Soc.* 2011, **126**, 11240; (b) D.-L. Long, E. Burkholder and L. Cronin, *Chem. Soc. Rev.* 2007, **36**, 105.
- (18) (a) J. M. Breen and W. Schmitt, *Angew. Chem. Int. Ed.* 2008, **47**, 6904; (b) J. M. Breen, R. Clérac, S. M. Cloonan, E. Kennedy, M. Feeney, T. McCabe, D. C. Williams and W. Schmitt, *Dalton Trans.* 2012, **41**, 2918; (c) S.-T. Zheng, J. Zhang, X.-X. Li, W.-H. Fang and G.-Y. Yang, *J. Am. Chem. Soc.* 2010, **132**, 15102.
- (19) Q. Chen and J. Zubieta, *Coord. Chem. Rev.* 1992, **114**, 107; (b) P. Song, W. Guan, L. Yan, C. Liu, C. Yao and Z. Su, *Dalton Trans.* 2010, **39**, 3706.
- (20) (a) D. D. Heinrich, K. Folting, W. E. Streib, J. C. Huffman and G. Christou, *J. Chem. Soc., Chem. Commun.* 1989, 1411; (b) J. Salta and J. Zubieta, *Inorg. Chim. Acta* 1996, **252**, 435; (c) W. Priebsch, D. Rehder and M. Von Oeynhausen, *Chem. Ber.* 1991, **124**, 761.
- (21) (a) X.-S. Wang, M. Chrzanowski, W.-Y. Gao, L. Wojtas, Y.-S. Chen, M. J. Zaworotko, and Ma, S. *Chem. Sci.* 2012, **3**, 2823; (b) D. J. Tranchemontagne, Z. Ni, M. O'Keeffe, O. M. Yaghi, *Angew. Chem. Int. Ed.* 2008, **47**, 5136.
- (22) S. R. Seidel and P. J. Stang, *Accounts Chem. Res.* 2002, **35**, 972.
- (23) M. Fujita, K. Umamoto, M. Yoshizawa, N. Fujita, T. Kusukawa and K. Biradha, *Chem. Commun.* 2001, 509.
- (24) D. Wulff-Molder and M. Meisel, *Acta Cryst.* 2000, **C56**, 33.
- (25) N. E. Brese and M. O'Keeffe, *Acta Cryst.* 1991, **B47**, 192.
- (26) G. B. Karet, Z. Sun, D. D. Heinrich, J. K. McCusker, K. Folting, W. E. Streib, J. C. Huffman, D. N. Hendrickson and G. Christou, *Inorg. Chem.* 1996, **35**, 6450.
- (27) F.-R. Dai, Z. Wang, *J. Am. Chem. Soc.* 2012, **127**, 8002.
- (28) Y.-S. Bae, K. L. Mulfort, H. Frost, P. Ryan, S. Punnathanam, L. J. Broadbelt, J. T. Hupp and R. Q. Snurr, *Langmuir* 2008, **24**, 8592.
- (29) Y. Yokomori, K. A. Flaherty and D. J. Hodgson, *Inorg. Chem.* 1988, **27**, 2300.